International Journal of Scientific Research and Engineering Development-– Volume 9 Issue 5, Sep-Oct 2026
Available at www.ijsred.com

RESEARCH ARTICLE OPEN ACCESS

Passive Islanding Detection for PV-Based Microgrids Using Sequence-Component Indices

Naveen Kumar[1], Prakash Narayan Tiwari[2]
[1,2]Department of Electrical and Electronics Engineering, Rabindranath Tagore University, Bhopal, India
DOI : https://doi.org/10.5281/zenodo.23940693

Abstract—
Unintentional islanding of distributed generators (DGs) endangers equipment and line workers, and the interconnection standard requires it to be detected within 2 s. This paper develops two passive detection indices based on sequence components measured at the point of common coupling (PCC). The first, RMPNSVC, is the ratio of the product of positive- and negative-sequence voltage to the product of positive- and negative-sequence current. The second, PAPSV, is the phase angle of the positive-sequence voltage evaluated every half cycle. Both were tested in MATLAB/Simulink on a distribution system with three photovoltaic (PV) DGs against zero, active and reactive power mismatch islanding, DG disconnection, line-to-ground, line-to-line and three-phase faults, and load, capacitor, inductor and motor switching. RMPNSVC separated the cases with a fixed threshold of 20 and detected islanding within 60 ms. PAPSV, with a threshold of 1.966°, detected islanding at zero mismatch in 0.10 s and in 7.82 ms at a 1.048 MW mismatch, and did not trip in any non-islanding case. No non-detection zone was found in the tested cases, and no signal is injected into the grid. The narrow threshold margin of PAPSV and the simulation-only validation are discussed.

***Index Terms*—Islanding detection, microgrid, photovoltaic, sequence components, non-detection zone, passive technique.**

I. INTRODUCTION

Renewable-based distributed generation is increasingly connected at distribution level, and microgrids built from such sources can operate connected to the utility or separated from it. When a fault or switching action cuts a part of the network from the utility and the DGs keep supplying it, an unintentional island is formed. In the island, voltage and frequency are no longer controlled by the utility, reclosing can occur out of phase, and repair crews may find conductors still energised. IEEE Std 1547-2018 therefore requires the DG to detect islanding and stop energising within 2 s [1].

Detection schemes are normally rated on speed, reliability during non-islanding events and the size of the non-detection zone (NDZ), the range of generation–load mismatch in which the island cannot be distinguished from normal operation [2]. Passive schemes measure voltage, frequency, harmonic content or phase quantities at the DG terminals and compare them with thresholds. They do not disturb the grid, but their NDZ and threshold sensitivity are a concern. Over/under-voltage and over/under-frequency relays have a large NDZ when the load depends on voltage and frequency [3], and ROCOF relays need a considerable power mismatch to operate [4]. Sequence components of voltage and current respond to unbalance and phase shifts and have given fast detection with small NDZ [5], [6], [7].

This paper presents two passive indices built on sequence components and evaluates them on a PV-based distribution system. The contributions are: (i) the RMPNSVC index and its threshold; (ii) the PAPSV index evaluated at half-cycle intervals; (iii) a test programme covering power-mismatch islanding, DG disconnection, faults and switching; and (iv) a comparison with published methods and a discussion of the threshold margin. The preliminary versions of the two indices were presented in [8] and [9].

II. RELATED WORK

Passive methods based on the rate of change of power [10], voltage unbalance with total harmonic distortion of current [11], the angle between negative-sequence voltage and current and the dq0 transformation [12] detect islanding within a quarter to half a cycle. Modal components [13], the rate of change of reactive power [14] and Pearson's correlation of micro-PMU data [15] extend this line. Active methods, such as frequency drift [16], [17], slip-frequency shift [18], current disturbance [19] and high-frequency impedance [20], have small NDZ but inject a disturbance that can degrade power quality. Hybrid schemes combine the two [21], [22], and remote schemes based on power-line signalling or transfer trip are reliable but expensive [23], [24]. The indices proposed here belong to the passive class and aim to keep its harmlessness to power quality while narrowing the NDZ.

III. SYSTEM UNDER STUDY

Fig. 1 shows the test network. Three PV-based DGs (DG1–DG3) of 15 kW each are connected through transformers to a 25 kV distribution system supplied by a 120 kV utility source through a 25 MVA, 120/25 kV transformer. Three 20 km π-section lines (DL1–DL3) connect the buses, loads L1–L4 are supplied at the nodes, and circuit breakers CB1–CB5 provide isolation. CB1 sits at the PCC: when it is open, the part of the network inside the dashed boundary is an island fed only by the DGs. The system frequency is 50 Hz, and three-phase voltage and current are sampled at 1 kHz. Each 15 kW DG is made of six 2.5 kW PV arrays with incremental-conductance maximum power point tracking, a boost converter and a PWM grid-tied inverter. A phase-locked loop based on Park's transformation, with sequence separation so that only the positive sequence is applied, keeps the inverter synchronised under unsymmetrical conditions. The model was built in MATLAB R2016a.

 ©IJSRED: All Rights are Reserved

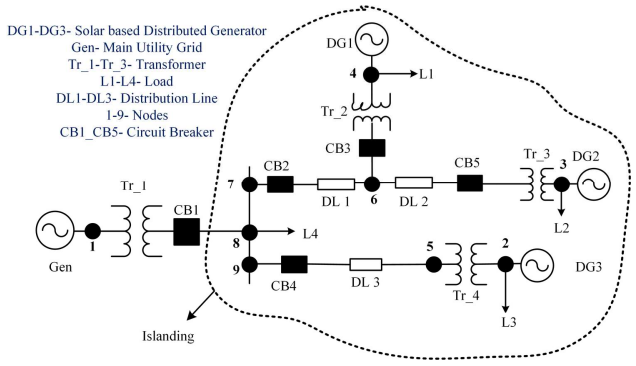


Fig. 1. Test distribution system with three PV-based DGs. CB1 at the PCC separates the island (dashed boundary) from the utility.

Islanding is created by opening CB1 at a chosen instant. Non-islanding events are created with the other breakers: faults and load switching at the PCC, DG disconnection and capacitor or inductor connection. For the PAPSV study the events are applied at t = 10.0 s, after the system has settled, and the power mismatch is expressed in MW and Mvar.

IV. PROPOSED DETECTION INDICES

A. Sequence components

The three-phase voltages and currents at the PCC are converted to sequence components with the Fortescue transformation,

$$V_1 = (V_a + aV_b + a^2V_c)/3 \quad (1)$$

$$V_2 = (V_a + a^2V_b + aV_c)/3 \quad (2)$$

with $a = 1\angle 120°$, and likewise for the currents I_1 and I_2. In grid-connected operation the voltage and current at the PCC are nearly balanced, so the negative-sequence components are small; an island, and unbalanced events, change the sequence quantities in different ways, and this is what the two indices exploit.

B. RMPNSVC index

The first index is the ratio of the product of positive- and negative-sequence voltage to the product of positive- and negative-sequence current,

$$\text{RMPNSVC} = (V_1 \times V_2)/(I_1 \times I_2) \quad (3)$$

and islanding is declared when RMPNSVC exceeds a threshold T. In the simulations the smallest value reached in an island, in the zero-mismatch case, was 50, whereas the largest value in any non-islanding event was below 0.01. A threshold $T = 20$ therefore leaves a large margin on both sides and was kept constant for all cases. Fig. 2(a) shows the flowchart.

C. PAPSV index

The second index is the phase angle of the positive-sequence voltage at the point of interconnection,

$$\text{PAPSV} = \arg(V_1) \quad (4)$$

computed with the sequence analyser block and monitored at every half cycle. Islanding is declared when

$$\text{PAPSV}_{calc} \geq \text{PAPSV}_{thr} \quad (5)$$

The index is close to zero in grid-connected operation (about 0.09° in the study) and increases during islanding and abnormal events. The threshold $\text{PAPSV}_{thr} = 1.966°$ was selected so as to separate the islanding and non-islanding cases that were simulated; for another network it would have to be re-determined from studies covering islanding at different mismatches and the usual disturbances. Fig. 2(b) gives the flowchart.

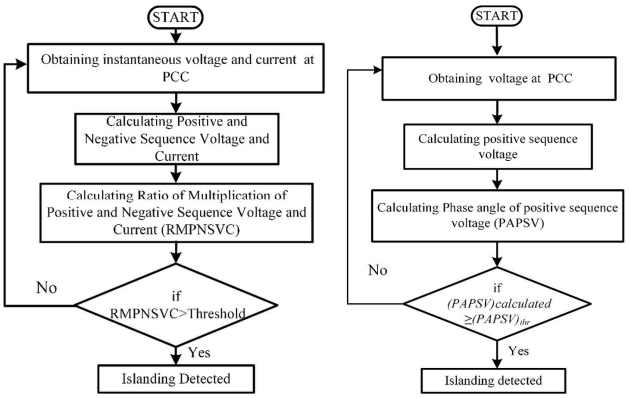


Fig. 2. Flowcharts of (a) the RMPNSVC technique and (b) the PAPSV technique.

V. RESULTS

A. RMPNSVC: islanding cases

All RMPNSVC tests opened CB1 at 0.5 s. For zero power mismatch (generation and load both 45 kW) the index was below the threshold before 0.5 s, crossed it after CB1 opened and produced a trip signal within 60 ms, as in Fig. 3(a); the NDZ was therefore not observed at balance. The load was then changed by +20%, +50%, −20% and −50% in turn, first the active and then the reactive part, because real loads vary over the day and the season. In all eight cases the trip signal was generated within 60 ms and no false signal appeared before CB1 was opened. Finally, DG3 was disconnected with its breaker at the same instant as CB1 opened; the index crossed the threshold at 0.56 s, again 60 ms after the event, as in Fig. 3(b).

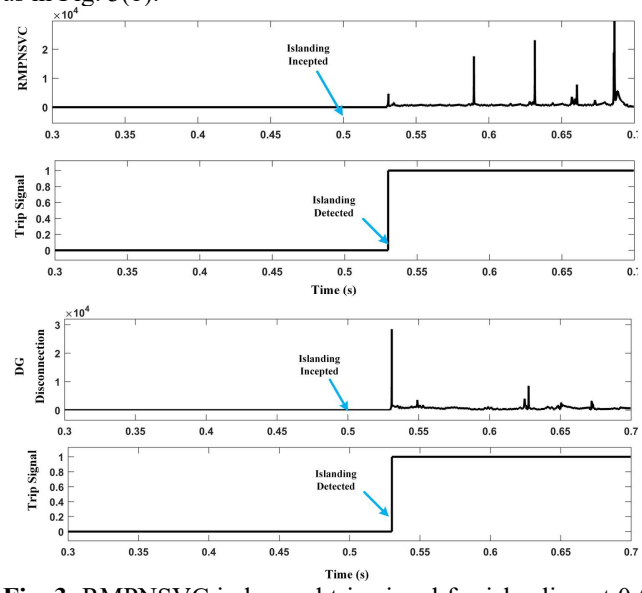


Fig. 3. RMPNSVC index and trip signal for islanding at 0.5 s: (top) zero power mismatch; (bottom) DG3 disconnection with CB1 open.

B. RMPNSVC: non-islanding cases

Line-to-ground (LG), double-line-to-ground (LLG) and three-phase (LLLG) faults with 1 Ω fault resistance were applied at the PCC at 0.5 s. After inception the index changed only slightly and never reached the threshold, so no trip signal was generated (Fig. 4, top, shows LLLG). A 1.5 kVAr inductor bank and a 1.5 kVAr capacitor bank were each switched at the PCC at 0.5 s; the index stayed below the threshold for the whole simulation (Fig. 4, bottom). The method is therefore stable for these events. Its main drawback

 ©IJSRED: All Rights are Reserved

is that the relay must resolve very small values, because the non-islanding index is close to zero.

TABLE I RMPNSVC RESULTS

Event	Setting	Outcome
Zero mismatch	45 kW load = 45 kW DG	Trip ≤ 60 ms
Active mismatch	+20%, +50%, −20%, −50%	Trip ≤ 60 ms (all)
Reactive mismatch	+20%, +50%, −20%, −50%	Trip ≤ 60 ms (all)
DG disconnection	DG3 opened with CB1	Trip at 60 ms
LG, LLG, LLLG fault	1 Ω at PCC	No trip
Inductor / capacitor	1.5 kVAr each	No trip

C. PAPSV: islanding cases

For zero power mismatch, with active and reactive mismatch within ±0.05 kW and ±0.05 kvar, the largest PAPSV was 2.073°, above the threshold, and a trip signal was issued after 0.10 s (Fig. 5, top). For a large mismatch of 1.048 MW and 1.028 Mvar between DG and load the peak was 2.665° and the detection time was 7.82 ms. As expected for a phase-based index, a larger mismatch moves the index further beyond the threshold and shortens the time to detect.

D. PAPSV: non-islanding cases

Load injection and ejection of 0.90 MW and 0.990 Mvar gave peaks of 1.668° and 1.559°. A 1.3 Mvar capacitor bank switched in and out gave peaks of 1.293° and 1.142°, and a 0.2 MW induction motor switched in and out gave 1.465° and 0.369°. Single-line-to-ground, double-line-to-ground, three-phase-to-ground, line-to-line and three-line faults, applied with 150 Ω fault resistance for 40 ms, gave peaks of 0.327°, 0.899°, 1.334°, 0.702° and 1.329°. All of them are below 1.966°, so every non-islanding event was classified correctly (Table II).

TABLE II PAPSV RESULTS (THRESHOLD 1.966°)

Event	Peak PAPSV (°)	Decision
Zero mismatch	2.073	Island, 0.10 s
1.048 MW / 1.028 Mvar	2.665	Island, 7.82 ms
Load in / out	1.668 / 1.559	No trip
Capacitor in / out	1.293 / 1.142	No trip
Motor in / out	1.465 / 0.369	No trip
LG, LLG, LLLG	0.327, 0.899, 1.334	No trip
LL, LLL	0.702, 1.329	No trip

VI. COMPARISON AND DISCUSSION

Three points should be kept in mind. First, the two indices differ in their threshold margin. The RMPNSVC threshold of 20 lies between a non-islanding maximum below 0.01 and an islanding minimum of 50, a very wide gap. The PAPSV threshold of 1.966° lies between a non-islanding maximum of 1.668° and an islanding minimum of 2.073°, a gap of only about 0.4° in which the threshold is closer to the islanding side by 0.1° and to the non-islanding side by 0.3°. A different network, measurement noise or a stronger load-switching event could close this margin, so PAPSV needs adaptive thresholding or further tests before field use. Second, RMPNSVC depends on very small non-islanding values, so the sensing chain and relay resolution must be adequate. Third, all results come from simulation of a PV-based system with fixed thresholds and without measurement noise or a hardware test, and the NDZ results apply only to the mismatches that were simulated. Both indices are passive and add no disturbance, so power quality is unaffected and several DGs cannot interfere with each other.

VII. CONCLUSION

Two passive islanding detection indices based on sequence components were developed and tested on a distribution system with three PV-based DGs. RMPNSVC detected islanding within 60 ms for zero, ±20% and ±50% active and reactive mismatch and for DG disconnection, and did not trip for faults and switching. PAPSV detected islanding at zero mismatch in 0.10 s and at a 1.048 MW mismatch in 7.82 ms, and stayed below its 1.966° threshold for load, capacitor, motor and fault events. Both detection times are far below the 2 s limit of IEEE 1547 [1], and no NDZ was observed in the tested cases. Future work should examine measurement noise and harmonics, multiple DGs with different technologies, adaptive thresholds, particularly for PAPSV, and validation with real-time simulation or laboratory hardware.

REFERENCES

[1] Ekta Purwar and K. Nagarjuna, “Improvement of Grid Resiliency During High Penetration of Smart Grid Renewable Resources Using Coordinated Protection and Control Strategies, Electric Energy Systems, now publishers inc; Boston.

[2] M. E. Ropp, M. Begovic, A. Rohatgi, G. A. Kern, R. H. Bonn, and S. Gonzalez, “Determining the relative effectiveness of islanding detection methods using phase criteria and nondetection zones,” IEEE Trans. Energy Convers., vol. 15, no. 3, pp. 290–296, Sep. 2000.

[3] A. Priyadarshi, K. B. Yadav, and V. Rathore, “Synchrophasor assisted load frequency control of interconnected system with multiple fuel inputs using honey badger algorithm,” Int. J. Model., Identification Control, vol. 43, no. 1, pp. 54–63, 2023.

[4] W. Freitas, W. Xu, C. M. Affonso, and Z. Huang, “Comparative analysis between ROCOF and vector surge relays for distributed generation applications,” IEEE Trans. Power Del., vol. 20, no. 2, pp. 1315–1324, Apr. 2005.

[5] J. Bashir, P. Jena, and A. K. Pradhan, “Islanding detection of a distributed generation system using angle between negative sequence voltage and current,” in Proc. 18th Nat. Power Syst. Conf. (NPSC), Guwahati, India, 2014, pp. 1–5.

[6] A.K and K Prasad,“Renewable Energy Sources Integration with Flywheel Energy Storage System based on Wind and Solar Energy, 2022 IEEE International Conference on Current Development in Engineering and Technology (CCET).

[7] M. Kumar and J. Kumar, “Islanding event detection technique based on change in apparent power in microgrid environment,” Electr. Eng., 2023

 ©IJSRED: All Rights are Reserved

[8] S. Shankar, K. B. Yadav, A. Priyadarshi, and V. Rathore, "Study of phasor measurement unit and its applications," in Recent Advances in Power Systems: Select Proc. EPREC 2020. Singapore: Springer, 2020, pp. 247–257.
[9] K. B. Yadav, and V. Kumar, "Modeling and simulation of micro-grid system components," in Proc. Int. Conf. Adv. Electron., Elect. Comput. Intell. (ICAEEC), IIIT Allahabad, India, Apr. 2019.
[10] M. A. Redfern, O. Usta, and G. Fielding, "Protection against loss of utility grid supply for a dispersed storage and generation unit," IEEE Trans. Power Del., vol. 8, no. 3, pp. 948–954, Jul. 1993.
[11] S.-I. Jang and K.-H. Kim, "An islanding detection method for distributed generations using voltage unbalance and total harmonic distortion of current," IEEE Trans. Power Del., vol. 19, no. 2, pp. 745–752, Apr. 2004.
[12] K. Sareen, B. R. Bhalja, and R. P. Maheshwari, "A new islanding detection technique for distribution system during DG interconnections," in Proc. IEEE ISGT Asia, Bangkok, Thailand, 2015, pp. 1–5.
[13] A Dixit and P Tiwari, Pattern and Prediction Analysis by Using Different Data Mining Techniques, Application of Advance Techniques in Power and Energy Systems: Select Proceedings of International Conference, CISTEE 2023.
[14] S.Nikolovski, H. R. Baghaee, and D. Mlakic, "Islanding detection of synchronous generator-based DGs using rate of change of reactive power," IEEE Syst. J., vol. 13, no. 4, pp. 4344–4354, Dec. 2019.
[15] G. P. Kumar and P. Jena, "Pearson's correlation coefficient for islanding detection using micro-PMU measurements," IEEE Syst. J., vol. 15, no. 4, pp. 5078–5089, Dec. 2021.
[16] Y. Jung, J. Choi, B. Yu, J. So, G. Yu, and J. Choi, "A novel active frequency drift method of islanding prevention for the grid-connected photovoltaic inverter," in Proc. IEEE 36th Power Electron. Spec. Conf. (PESC), Recife, Brazil, 2005, pp. 1915–1921.
[17] A. Yafaoui, B. Wu, and S. Kouro, "Improved active frequency drift anti-islanding detection method for grid connected photovoltaic systems," IEEE Trans. Power Electron., vol. 27, no. 5, pp. 2367–2375, May 2012.
[18] P. K. Ganivada and P. Jena, "Active slip frequency based islanding detection technique for grid-tied inverters," IEEE Trans. Ind. Informat., vol. 16, no. 7, pp. 4615–4626, Jul. 2020.
[19] P. Li, Y. Sheng, L. Zhang, X. Yang, and Y. Zhao, "A novel active islanding detection method based on current-disturbing," in Proc. Int. Conf. Elect. Mach. Syst. (ICEMS), Tokyo, Japan, 2009, pp. 1–5.
[20] K. Jia, H. Wei, T. Bi, D. W. P. Thomas, and M. Sumner, "An islanding detection method for multi-DG systems based on high-frequency impedance estimation," IEEE Trans. Sustain. Energy, vol. 8, no. 1, pp. 74–83, Jan. 2017.
[21] G. Wang, F. Gao, and J. Liu, "A hybrid islanding detection method combining VU/THD and BRPV," in Proc. IEEE Energy Convers. Congr. Expo. (ECCE), Portland, OR, USA, 2018, pp. 3682–3687.
[22] P. Tiwari K. Thakre , "Performance Analysis of PV Fed DC-DC Converter for Simultaneous Buck-Boost Operation", 2022 IEEE International Conference on Current Development in Engineering and Technology (CCET).
[23] A. Bharatee, M. Mishra, and B. B. Pati, "Anti-islanding protection by power line signaling and wavelet transform," in Proc. Global Conf. Advancement Technol. (GCAT), Bengaluru, India, 2019, pp. 1–5.
[24] R. A. Walling, "Application of direct transfer trip for prevention of DG islanding," in *Proc. IEEE Power Energy Soc. Gen. Meeting*, Detroit, MI, USA, 2011, pp. 1–3.
[25] P.Tiwari, A Dixit "The, Application of Advance Techniques in Power and Energy Systems: Select Proceedings of International Conference, CISTEE 2023
[26] M. Seyedi, S. A. Taher, B. Ganji, and J. Guerrero, "A hybrid islanding detection method based on the rates of changes in voltage and active power for the multi-inverter systems," *IEEE Trans. Smart Grid*, vol. 12, no. 4, pp. 2800–2811, Jul. 2021.
[27] K. Prasad and K. Thakre," Control of hybrid standalone power supply system using artificial neural network, Majlesi Journal of Electrical Engineering.
[28] A. Raghuwanshi, D. Kumar, and S. Gupta, "Load frequency control of multisource interconnected system using a nature-inspired optimization algorithm," in Proc. IEEE Region 10 Conf. (TENCON 2025), Malaysia, Oct. 2025, pp. 850–854
[29] P. Gupta, R. S. Bhatia, and D. K. Jain, "Active ROCOF relay for islanding detection," IEEE Trans. Power Del., vol. 32, no. 1, pp. 420–429, Feb. 2017.
[30] Bhavesh R. Bhalja and O. P. Malik "Novel Hybrid Framework for Detection, Discrimination, and Classification of Stator Winding Faults in Induction Motors, IEEE Transactions on Industry Application Pages: 2572-2586, Volumes: 62.

.

 ©IJSRED: All Rights are Reserved